Understanding Macroscopic Diffusion of Adsorbed Molecules in Crystalline Nanoporous Materials via Atomistic Simulations

DAVID S. SHOLL*

Department of Chemical Engineering, Carnegie Mellon University, Pittsburgh, Pennsylvania 15213

Received December 15, 2005

ABSTRACT

The diffusion rates of molecules inside nanoporous materials lie at the heart of many large-scale industrial applications of these materials. Quantitatively describing this diffusion, particularly diffusion of chemical mixtures in situations leading to net mass transport, remains challenging. Molecular dynamics (MD) simulations can play an important complementary role to experiments in this area. This Account describes applications of MD to diffusion in nanoporous materials with a particular focus on macroscopic diffusion, that is, diffusion involving mass transport. These methods have made useful contributions to developing mixing theories for predicting multicomponent diffusion from single-component data and to screening new classes of materials for practical applications.

Introduction

The nanometer-scale pores in materials such as zeolites and activated carbons have useful properties that form the basis of large-scale industrial processes such as pressure swing adsorption (PSA) for gas separations and shape-selective catalysis for petroleum refining.[1,2] These materials are traditionally referred to as microporous,[1,2] although calling them nanoporous is linguistically accurate and more descriptive. In this Account, I discuss a deceptively simple question: how fast do molecules diffuse inside ordered nanoporous materials? This question has a long history.[1−4] Recently, atomically detailed simulations have provided a useful complement to experimental approaches. My purpose here is to describe how simulations can describe macroscopic diffusion in nanoporous crystals.

Why is diffusion in nanopores still an active field? Nanoporous materials form the core of a wide range of industrial processes. Often, processes are operated on the basis of equilibrium adsorption selectivity.[1] In these cases, diffusion is only relevant if it limits the achievable cycle times. In other examples, however, diffusivity differences are integral to the process. Kinetics-based PSA separation is one example.[1] Membrane-based separations intrinsically rely on a combination of adsorption and diffusion properties.[5−7] To advance these applications, diffusion of chemical mixtures must be understood. Mixture diffusion is not a trivial extension of single-component diffusion.[8] Unfortunately, experimental characterization of mixture diffusion in nanopores is challenging. Even measuring single-component diffusion in nanopores experimentally is often controversial, with different techniques giving enormously different results.[2−4] Atomistic simulations can assist in explaining the origins of these controversies and give much needed insight into mixture diffusion.

I restrict my attention to simulations with an atomistic model of the nanoporous adsorbents. An alternative approach is to use lattice models, which are extremely useful in studying the phenomenology of diffusion.[9,10] Lattice models can give quantitative insight,[11] but it is difficult to derive lattice models that quantitatively describe all properties of real adsorbents.

An especially useful role for detailed simulations lies in screening new materials for potential applications. One goal of this Account is to demonstrate how validation of simulation methods for well-known materials has led to opportunities to guide material development with newer materials including carbon nanotubes and metal organic frameworks (MOFs).

Single-Component Diffusion—Definitions

The quantities associated with molecular diffusion have been carefully defined in numerous sources,[2,3,12] but for clarity, it is important to reiterate them here. The central concept to grasp is that diffusion is defined by *multiple* diffusion coefficients describing different aspects of mass transport. Figure 1 shows data for ethane diffusion in silicalite. Before discussing this example in detail, it is vital to describe the multiple diffusion coefficients that appear in it.

First, consider a single-component chemical adsorbed inside an isotropic nanoporous crystal at a concentration c with the location of molecule i at time t denoted by $\vec{r}_i(t)$. Here, c is the density of molecules averaged over some volume large in length scale relative to the microscopic density variations that can occur within a unit cell of the adsorbent. When $\Delta\vec{r}_i$ is defined as $\Delta\vec{r}_i = \vec{r}_i(t) - \vec{r}_i(0)$ and the positions of N distinct molecules for time t are tracked, then

$$\frac{1}{N}\sum_{i=1}^{N}\Delta\vec{r}_i^{\,2} = 6D_s(c)t \text{ as } t \to \infty \qquad (1)$$

This expression defines the *self-diffusion coefficient*, $D_s(c)$ (also known as the tracer diffusion coefficient). This description is familiar to many chemists via the Stokes−Einstein description of particle mobilities in solution.[13]

David Sholl was born in 1969 in Armidale, New South Wales, Australia. After a B.S. (Honors) in theoretical physics at the Australian National University, he obtained a Ph.D. in applied mathematics from the University of Colorado. He is a Professor of Chemical Engineering with a courtesy appointment in Materials Science and Engineering at Carnegie Mellon University. In addition to diffusion in nanoporous materials, David works on the surface chemistry of metals and development of metal hydrides for hydrogen storage and purification.

* To whom correspondence should be addressed. Telephone: 412-268-4207. Fax: 412-268-7139. E-mail: sholl@andrew.cmu.edu.

10.1021/ar0402199 CCC: $33.50
Published on Web 03/29/2006

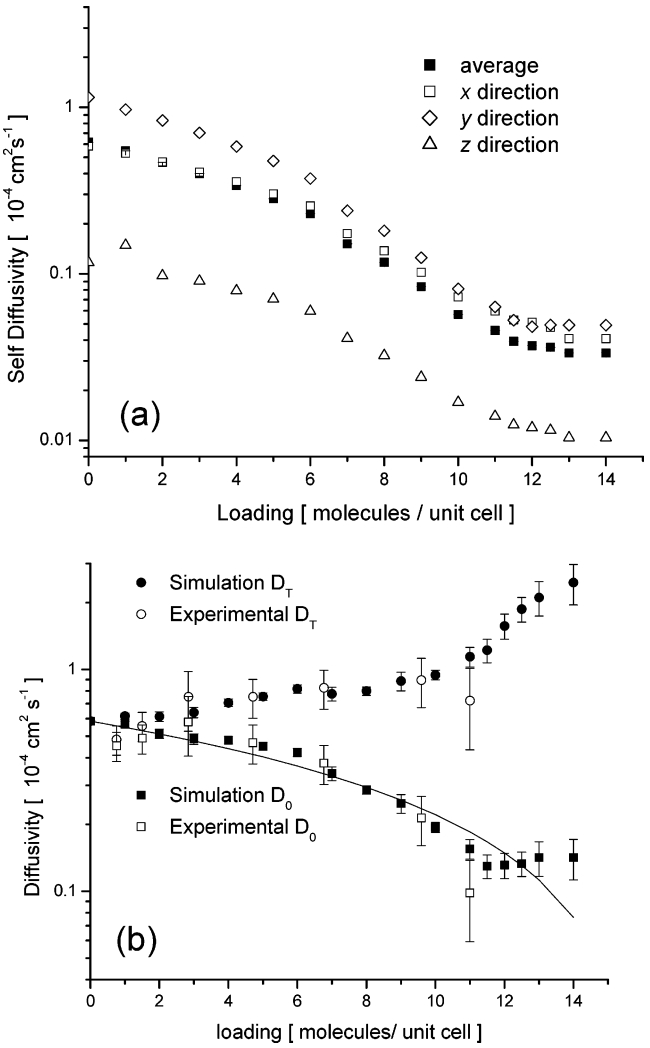

FIGURE 1. (a) Directional and orientationally averaged D_s for room-temperature ethane in silicalite from EMD. (b) Orientationally averaged transport and corrected diffusivities of ethane in silicalite from EMD (● and ■) and neutron scattering (○ and □). The solid curve shows D_0 from a noninteracting lattice model. The figure was reproduced with permission from ref 24.

Another, more macroscopic, definition of diffusion is based on the fact that a net flux occurs if a concentration gradient exists. This flux, $\vec{J}$, is given by Fick's law

$$\vec{J} = -D_t(c)\nabla c \tag{2}$$

defining the *transport diffusion coefficient* (also known as the Fickian or chemical diffusivity). In applications that involve net mass transfer, such as membranes, it is this diffusivity that is of interest. $D_s(c)$ and $D_t(c)$ are functions of the concentration and *are not equal*. In extreme examples, they differ by orders of magnitude. Analysis of diffusion must use the diffusivity appropriate for the application being considered.

One more diffusion coefficient is widely used in describing nanoporous materials. If the adsorption isotherm relating the adsorbed concentration to the bulk fugacity of the adsorbing species, f, is known, then D_t can be written without approximation as

$$D_t(c) = D_0(c)\frac{\mathrm{d}\ln f}{\mathrm{d}\ln c} \tag{3}$$

Here, $D_0(c)$ is the *corrected diffusion coefficient* (also known as the single-component Maxwell−Stefan diffusivity), and the derivative is the thermodynamic correction factor. A common empirical approximation is to assume $D_0(c)$ is independent of c. This is frequently referred to as the Darken approximation,[14] despite Darken's explicit assertion in his classic paper[15] that $D_0(c)$ is *not* constant as c varies! Efficient simulation techniques exist to calculate adsorption isotherms for atomistic models of nanoporous adsorbents.[16−18]

Molecular dynamics (MD) simulations offer an appealing way to characterize diffusion in nanopores because they generate the time-dependent trajectories of adsorbed particles, $\vec{r}_i(t)$. Self-diffusivities can be determined from MD using eq 1 or via velocity autocorrelation functions.[19] Many studies have used this approach to describe self-diffusion.[2,3] It is less obvious how to extract $D_t(c)$ from MD. This problem was elegantly addressed by Maginn et al., who examined several methods.[20] The approach that I shall highlight involves using equilibrium MD (EMD). From EMD, the corrected diffusion coefficient is[12,20,21]

$$\frac{1}{N}\left\langle\left[\sum_{i=1}^{N}\Delta r_i\right]^2\right\rangle = 6D_0(c)t \text{ as } t \to \infty \tag{4}$$

where N is the number of adsorbed molecules in the simulation volume and $\langle\ldots\rangle$ indicates an average over multiple independent trajectories. It can be helpful to think of eq 4 as describing the diffusive motion of the center of the molecules of mass relative to the reference frame of the adsorbent. With $D_0(c)$ given by eq 4, $D_t(c)$ is found using eq 3. Using EMD in this way, D_s, D_0, and D_t can be simultaneously calculated at an unambiguously defined adsorbate concentration. Other related simulation techniques exist using nonequilibrium MD or explicit concentration gradients.[20,22] These methods do not calculate all three diffusivities simultaneously, although they may be more numerically efficient than EMD in some instances.[23]

The three diffusivities defined above coincide in one important limit;[2,3] at low adsorbate concentrations, the self-, transport, and corrected diffusivities are equal. This follows directly from eqs 1, 3, and 4. It is useful to denote this dilute concentration diffusivity by $D(0)$; therefore,

$$\lim_{c\to 0} D_s(c) = \lim_{c\to 0} D_t(c) = \lim_{c\to 0} D_0(c) = D(0) \tag{5}$$

Single-Component Diffusion—Examples

To illustrate EMD simulations of macroscopic diffusion in nanopores, I will describe a series of examples dealing with all-silica zeolites. Figure 1 shows the concentration-dependent diffusivities of ethane in silicalite at room temperature.[24] Silicalite is the all-silica form of ZSM-5 (structure code MFI) and has been widely studied.[2,3] The simulations in Figure 1 used a united-atom model for ethane and defined ethane−zeolite interactions via a

Table 1. Comparison of Measurements and EMD Simulations of Ethane Diffusion in Silicalite at Room Temperature[a]

experimental method	quantity measured	loading (molecule/unit cell)	experimental value (10^{-4} cm^2/s)	simulation value (10^{-4} cm^2/s)
QENS[26]	D_s	1	0.2	0.549
		4	0.3	0.339
		8	0.125	0.117
PFG−NMR[27]	D_s	"low"	0.5	0.474
single-crystal membrane[28]	$D_{0,z}$	1	0.113	0.165

[a] All self-diffusivities are orientationally averaged. The table was reproduced with permission from ref 24. EMD data for the "low" loading was averaged between 1 and 4 molecules/unit cell.

Lennard−Jones potential. This potential was parametrized to fit experimental adsorption data.[16,17] The pores of silicalite are anisotropic; therefore, diffusion in silicalite is anisotropic, as shown in Figure 1a. Comparing the orientationally averaged self-, corrected, and transport diffusion coefficients in parts a and b of Figure 1 makes it clear that these three quantities are different. When there are 12 molecules/unit cell, D_t/D_s is >30. This situation does not require extreme conditions; the pressure needed to create this concentration is <10 bar.[17]

Figure 1b also shows measurements of the transport diffusivity of ethane using neutron scattering. Considering that no adjustable parameters existed when comparing the MD and experimental data, the agreement is remarkable. Similar agreement has been found for CF_4 diffusion in silicalite.[25]

Figure 1b shows that the corrected diffusivity of ethane decreases strongly with an increasing concentration. The empirical approximation that $D_0(c)$ is a constant is not quantitatively correct for this example. Another simple approximation for $D_0(c)$ is to describe the diffusion as occurring via particles hopping on a lattice with only hard-core interactions between particles. The resulting diffusivity is shown as a solid curve in Figure 1b; it captures the general features but not every detail of the actual diffusivity.

Because experimental measurements of diffusion in zeolites can be controversial,[4] it is best to compare simulations with multiple experiments. Table 1 compares ethane diffusivities in silicalite computed with EMD and multiple experimental measurements. The quasielastic neutron scattering (QENS)[26] and pulsed field-gradient nuclear magnetic resonance (NMR)[27] results in Table 1 measured orientationally averaged self-diffusion; the single-crystal membrane experiment[28] measured the z component of $D_0(c)$. Each MD result in Table 1 is for the same diffusion coefficient at the same ethane concentration as the corresponding experiment. The multiple experimental methods gave results that are self-consistent, and the EMD calculations are in excellent agreement with the experiments. The increase in D_s going from 1 to 4 molecules in the QENS experiments in Table 1 is not seen in the EMD results. This discrepancy may arise from a low concentration of Na cations in the experiments.[24]

One useful way to use MD is to explore how pore structure and connectivity affect diffusion.[14,29,30] Figures 2 and 3 show examples of room-temperature diffusivities computed for three all-silica zeolites: silicalite, ITQ-3, and ZSM-12.[30] Silicalite has a 3D pore structure with pores roughly 0.5 nm in diameter. ITQ-3 consists of cages separated by windows with diameters of roughly 0.4 nm.

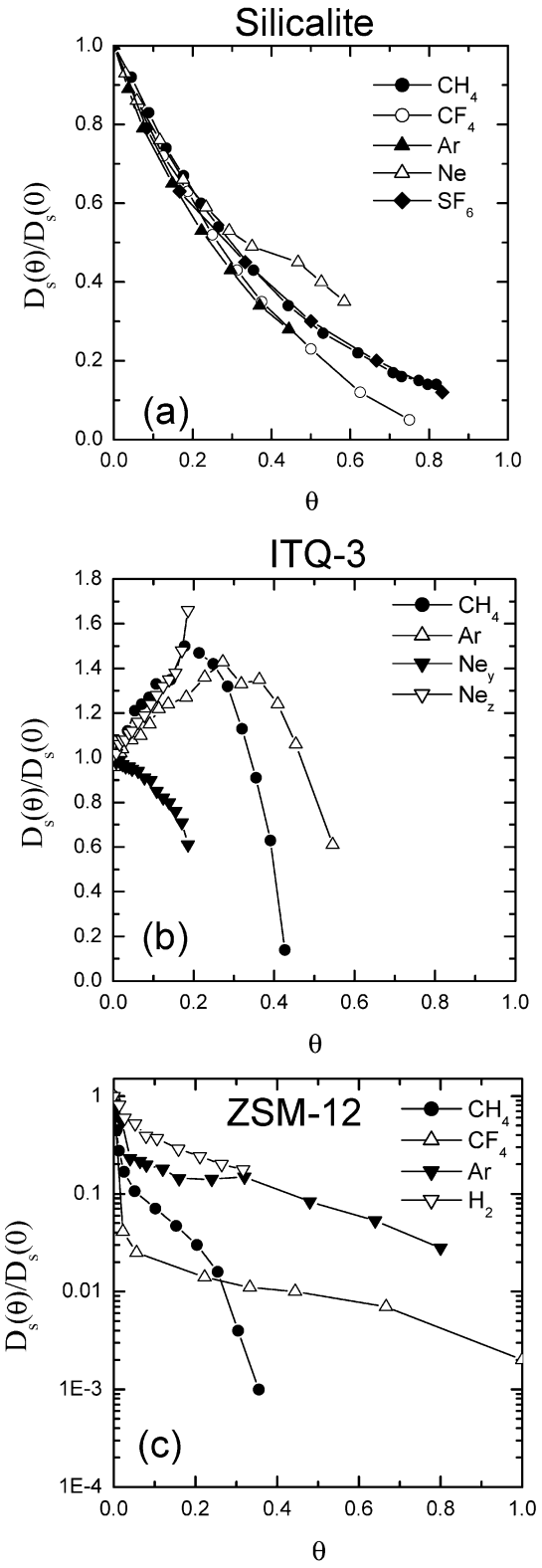

FIGURE 2. Concentration dependence of D_s from EMD for (a) silicalite, (b) ITQ-3, and (c) ZSM-12. The figure was reproduced with permission from ref 30.

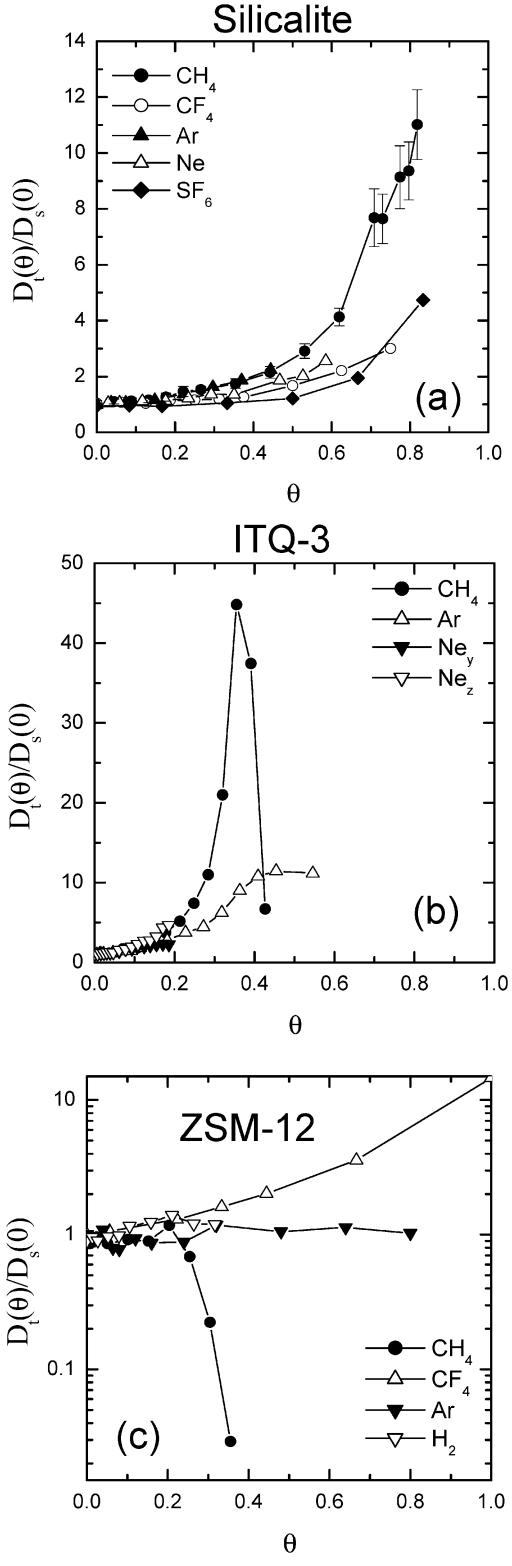

FIGURE 3. Same as Figure 2 but showing D_t (with different vertical scales than Figure 2). The figure was reproduced with permission from ref 30.

ZSM-12 has pores similar in diameter to silicalite, but these pores are unidimensional. In each figure, the diffusivities are normalized by the dilute loading value from eq 5, $D(0)$, and the loading is normalized by the saturation loading from the adsorption isotherm. Of the species simulated in ITQ-3, only Ne can diffuse in both the y and z directions, and these diffusivities are shown separately.

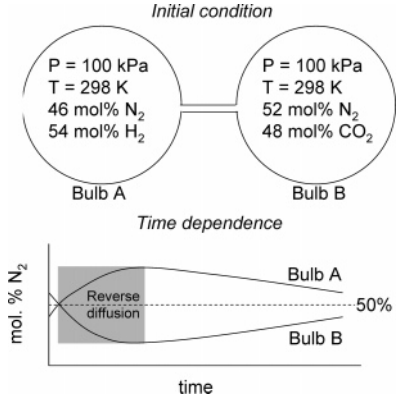

FIGURE 4. Schematic illustration of the Duncan and Toor experiment,[41] adapted from ref 40. Mixing occurs only by diffusion. The evolution of the N_2 concentration in each bulb is shown.

Figures 2 and 3 show a diverse range of behaviors. This general observation has been made before from experiments with self-diffusion in zeolites.[3] The maxima for $D_s(c)$ in ITQ-3 occur because, at low concentrations, adsorbate–adsorbate interactions reduce the effective barrier to hopping between cages.[30,31] The rapid decrease in $D_s(c)$ for low concentrations of the larger molecules in ZSM-12 occurs because it is difficult for molecules to pass one another in these unidimensional pores. This behavior is related to single-file diffusion, the situation when molecules cannot pass one another in unidimensional pores.[32–34]

Several observations can be made from the transport diffusivities in Figure 3. Considering only CH_4 shows that $D_t(c)$ can strongly increase, strongly decrease, or be nonmonotonic as a function of the concentration. The transport diffusivities can be very different from the self-diffusivities at moderate and high adsorbate concentrations. For example, $D_t(c)/D_s(c)$ is roughly 100 for CH_4 in silicalite at the highest concentrations shown in Figures 2 and 3. The existence of situations such as this for a simple molecule inside a material that is (at least chemically speaking) relatively simple emphasizes the fact that studies of diffusion in nanopores must carefully account for the type of diffusion being measured.

Motivated in part by the results above, the use of MD simulations to predict macroscopic diffusivities in nanopores is rapidly becoming part of the standard suite of calculations that can be applied to an atomically detailed model of an adsorbate/adsorbent pair of interest. Single-component diffusion of a wide range of adsorbates in silica zeolites has now been studied in this way.[23,35–39]

Diffusion of Chemical Mixtures

Almost all applications of diffusion in nanopores involve chemical mixtures. To appreciate that eq 2 cannot describe mixture diffusion, it is useful to consider a beautiful experiment performed almost 50 years ago.[40,41] This experiment, illustrated in Figure 4, creates an highly ideal gas mixture that mixes via diffusion. For a considerable

period during this mixing, N_2 diffuses against its concentration gradient. This striking example demonstrates that any description of mixture diffusion must account for diffusion of one species induced by inhomogeneity in other species. Several mathematically equivalent formalisms accomplish this task.[40,42] Irreversible thermodynamics expresses the species fluxes in terms of chemical potential gradients

$$\vec{J}_i = -\sum_{j=1\rightarrow N} L_{ij}(\mu_1, ..., \mu_N)\nabla\mu_j \qquad (6)$$

Here, L_{ij} is the symmetric matrix of Onsager transport coefficients. An equivalent description relates the fluxes to concentration gradients

$$\vec{J}_i = -\sum_{j=1\rightarrow N} D_{ij}(c_1, ..., c_N)\nabla c_j \qquad (7)$$

Here, the diffusion coefficients, D_{ij}, are not symmetric. I will refer to this matrix as the binary transport diffusivities, [D]. [L] and [D] are related (without approximation) by expressions involving derivatives of the equation of state of the mixture (that is, the mixture adsorption isotherm for adsorbed species).[42,43] Mixture isotherms can be accurately characterized from an atomistic description of adsorbents.[16−18]

A third formalism for mixture diffusion is the Maxwell−Stefan description.[40] Maxwell−Stefan diffusivities can also be related without approximation to [L] or [D]. None of these three formalisms is more "correct" than the other; they are all mathematically equivalent. Choosing which formalism to use is a matter of convenience and not physical correctness.[40]

The matrix of diffusivities for mixtures depends upon the concentrations of all diffusing species; therefore, experimental characterization is challenging. Atomistic simulations can play an important role to complement experiments, because simulating mixtures is not particularly more difficult than simulating single components. The key observation is that eq 4 can be generalized to give [L] for an adsorbed mixture from EMD.[12] In EMD of an isotropic material in a volume V containing N_j molecules of species j where the kth molecule of species j has position $r_{k,j}(t)$

$$\frac{1}{VkT}\langle[\sum_{l=1}^{N_i}\Delta\vec{r}_{l,i}][\sum_{k=1}^{N_j}\Delta\vec{r}_{k,j}]\rangle = 6L_{ij}t \text{ as } t\rightarrow\infty \qquad (8)$$

The first systematic use of eq 8 was by Sanborn and Snurr,[44,45] who simulated CH_4/CF_4 mixture diffusion in all-silica faujasite. After this work, extensive simulations of other mixtures in all-silica zeolites have appeared.[23,35−37,43,46,47] Figure 5 shows examples of [D] computed using EMD for room-temperature CH_4/CF_4 mixtures in silicalite.[43] For convenience, CH_4 is denoted species 1 and CF_4 is denoted species 2. As a single component, CH_4 diffuses considerably faster than CF_4 under all conditions. For example, as $c\rightarrow 0$, $D_{CH_4}(0)/D_{CF_4}(0) > 3$.[29,30] For CF_4-rich mixtures, a composition appropriate for adsorption of CH_4/CF_4 mixtures,[46,48] the situation is quite different. For adsorbed mixtures that are 70% CF_4 with a total concentration of 14 molecules/unit cell, the largest component of [D] relates the CF_4 flux to gradients in the CF_4 (that is, D_{22}), while the element relating CH_4 flux to CH_4 gradients (D_{11}) is the smallest. The off-diagonal binary transport diffusivities (D_{12} and D_{21}) are comparable in size to the diagonal elements for this mixture. This specific example highlights the general observations that mixture diffusion in nanopores can be very different to single-component diffusion and that including matrix elements in eq 7 is vital to describe mixture diffusion quantitatively.

Predicting Mixture Diffusion from Single-Component Information

In practical applications, it is desirable to accurately describe mixture diffusion without having to perform experiments or simulations for all conceivable mixture compositions and concentrations. This is especially true for mixtures containing more than two components. It is reasonable to ask whether mixture diffusivities can be predicted using only single-component information. Various mixing theories of this type have been suggested,[43] but the scarcity of detailed experimental data for macroscopic mixture diffusion in nanopores limited efforts to test these theories. Perhaps the most important role to date for MD simulations of mixtures has been to provide data for the testing of diffusion mixing theories.

A mixing theory that appears promising was introduced by Skoulidas, Krishna, and myself after testing several approaches against EMD data for CH_4/CF_4 mixtures in silicalite.[43] The essence of this approach is to characterize single-component diffusion using the c-dependent self-*and* corrected diffusion coefficients, $D_s(c)$ and $D_0(c)$. Differences between these quantities contain information about correlation effects.[43] This theory also requires the binary adsorption isotherm. If only single-component information is to be used, the mixture isotherm can be predicted using the ideal adsorbed solution theory (IAST).[1,48] The theory combines these single-component properties using an empirical mixing rule to give the mixture diffusivities. Once the saturation loadings of the individual adsorbing species are established and appropriate continuous functions are found to fit the single-component diffusivities, this approach contains no adjustable parameters.

The predictions of this mixing theory for CH_4/CF_4 mixtures in silicalite are compared with EMD data in Figure 5. IAST was used to predict the binary adsorption isotherms, an accurate approach for this example.[48] Although the predictions of the this theory are not exact, they capture the quantitative trends in the EMD data with considerable accuracy. The only regime where the mixing theory is somewhat inaccurate is for the highest concentrations of the 30:70 mixture, where the theory predicts nonmonotonic behaviors in D_{21} and D_{22} that are not supported by the EMD data.

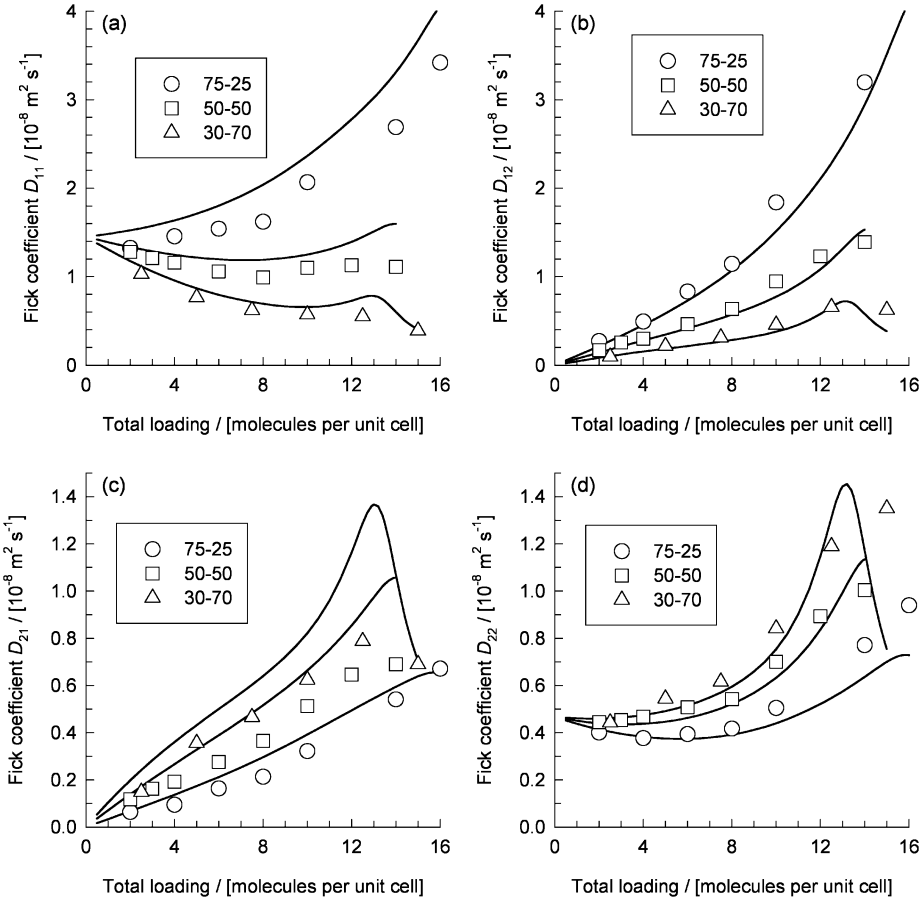

FIGURE 5. EMD results for [D] for room-temperature CH_4/CF_4 mixtures in silicalite, with results for mixtures that are 75:25 (○), 50:50 (□), and 30:70 (△) CH_4/CF_4. A subscript 1 refers to CH_4, and a subscript 2 refers to CF_4. Solid curves show predictions from the mixing theory described in the text. The figure was reproduced with permission from ref 43.

This mixing theory has subsequently been compared by Krishna and co-workers to EMD mixture diffusion data for hexane/butane isomers in mordenite[35] and linear alkanes in silicalite[37] and faujasite.[23,36] In all cases, including the small number of ternary and quaternary mixtures that have been examined,[36] the mixing theory is quantitatively accurate. Only one example is known where this mixing theory is inaccurate, a recent analysis of a two-dimensional lattice model heuristically describing diffusion in a material with strong site energy heterogeneity.[49] The available evidence, therefore, suggests that this mixing theory is accurate in some but not all situations. Future testing of the theory in a broad range of systems will be valuable for understanding when it can be reliably applied.

Screening New Materials Using Simulations

The number of known nanoporous materials is very large and continues to grow rapidly. Selecting the most promising examples for moving new materials from discovery to applications is an important challenge. This is particularly true in efforts to create membranes, because large time and resource investments are required for useful membranes, even when the synthesis of bulk particles is well-known. Atomistic simulations can play an important complementary role to experiments by making predictions prior to experimental studies. The goal of performing simulations in this context is not to make *precise* predictions; rather, it is to predict whether a new material is significantly different from known materials. In this section, I describe simulations of diffusion in two classes of nanoporous materials that were made prior to experiments being performed, single-walled carbon nanotubes (SWNTs) and MOFs.

The earliest simulations of diffusion inside SWNTs focused on self-diffusion at high adsorbate concentrations.[50] The resulting diffusivities were slightly larger than analogous results for zeolites. When simulations were performed to examine macroscopic diffusion, however, a very different result emerged. EMD simulations of gases diffusing inside defect-free SWNTs predicted transport diffusivities orders of magnitude larger than had been observed in any other porous material.[51] Diffusivities predicted by EMD simulations of CH_4 and H_2 adsorbed inside (10,10) SWNTs, as single components and mixtures, are shown in Figure 6, together with results for ZSM-12, a silica zeolite with one-dimensional channels.[51,52] At around the same time, Sokhan et al. observed rapid gas transport inside SWNTs in MD simulations examining hydrodynamic slip lengths.[53] Rapid macroscopic diffusion of a variety of light gases in SWNTs has now been characterized using MD.[51,52,54−56] Rapid diffusion of polymer-

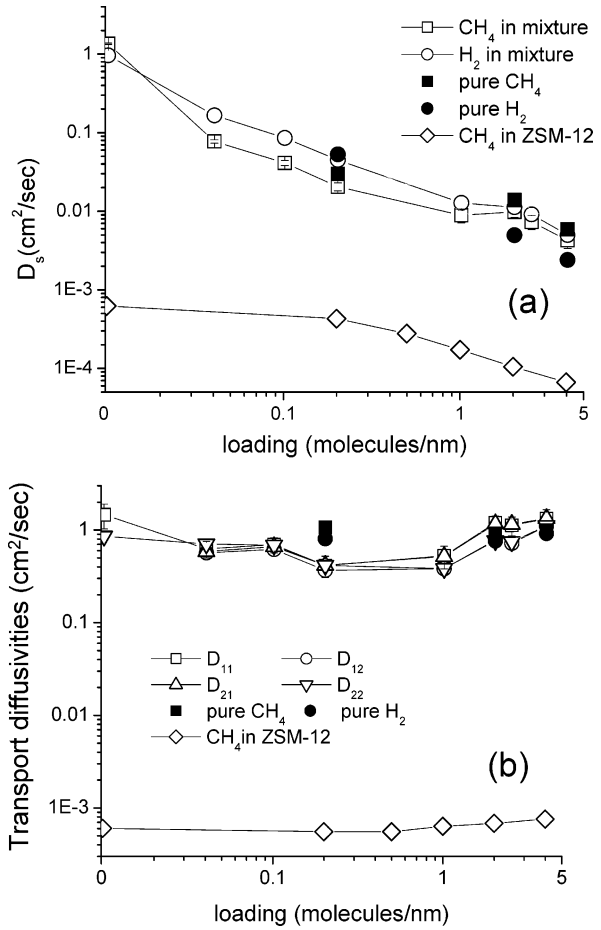

FIGURE 6. (a) D_s for single-component CH_4 and H_2 (■ and ●) and equimolar CH_4/H_2 mixtures (□ and ○) inside a (10,10) SWNT at room temperature, computed from EMD. (◇) Diffusion coefficient from EMD simulations of single-component CH_4 in ZSM-12. (b) Same as (a) but showing D_t. The figure was reproduced with permission from ref 52.

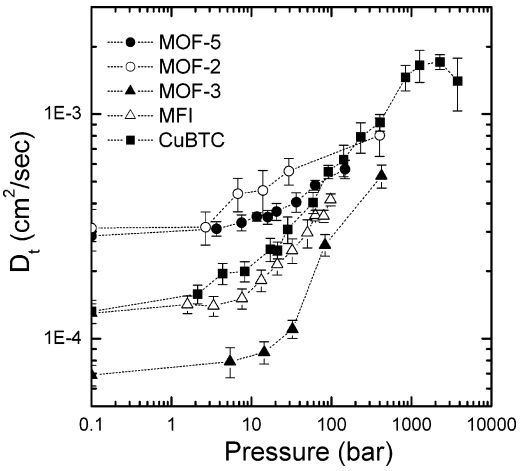

FIGURE 7. Single-component D_t computed using EMD for Ar diffusion at room temperature in four MOFs (MOF-5, MOF-2, MOF-3, and CuBTC) and in silicalite (MFI). The figure was reproduced with permission from ref 65.

like molecules has been observed in simulations of self-diffusion at low concentrations.[57]

These simulations predicted that diffusion inside SWNTs is *qualitatively* different than inside zeolites. This is possible because of the smoothness of SWNT walls on atomic scales; when a molecule collides with the wall, it undergoes near-specular reflection.[51,53,58] These simulations of course rely on several assumptions. In particular, adsorbate−wall interactions were defined by potentials appropriate for graphitic carbon, and SWNT walls were assumed to be rigid. The latter assumption has been carefully tested.[59,60] Including that the flexibility of the SWNT reduces the computed diffusivities, but this effect is quite small for nondilute adsorbate concentrations.

These results provide a strong motivation to tackle the challenge of fabricating SWNT membranes. Simulations of CH_4/H_2 mixtures suggest that SWNT membranes could exhibit significant selectivity for CH_4 and, more importantly, extraordinarily high transmembrane fluxes.[55] The fabrication of membranes that achieve both high fluxes and selectivities is a long-standing goal in the area of gas separations.[6] Recently, Hinds et al. have created membranes from multiwalled nanotubes that do indeed exhibit very high fluxes for single-component gases and liquids.[61,62]

Atomistic simulations have also been applied to gas diffusion in MOF materials. These materials are of great interest because, in part, their synthesis can be tuned to adjust their structure.[63] Although gas adsorption is routinely measured in MOFs,[64] to date, I know of no experimental data for gas diffusivities in MOFs. Figure 7 shows EMD predictions for the concentration dependence of $D_t(c)$ for Ar in four different MOFs and silicalite.[65] These calculations used interatomic potentials that are reasonably accurate for predicting single-component adsorption in these materials.[65] Similar calculations were performed for CH_4, CO_2, N_2, and H_2 in MOF-5,[65] and Sarkisov et al. used EMD to examine alkane self-diffusion at low concentrations in MOF-5.[66] These calculations indicate that molecular diffusivities in MOFs and zeolites are similar in magnitude. This observation is straightforward to understand by considering the pore volume readily accessible to adsorbates at thermal energies; the characteristics of this volume are similar to the interior of zeolite pores, even in MOFs that have very high porosities.[65,66] These results indicate that, in general, MOF membranes (if they were fabricated) would behave similarly to existing zeolite membranes. Specific applications may exist where MOF membranes will outperform existing membranes, but the motivation to create new membranes from MOFs should be based on quantitative arguments rather than the vague notion that they are "novel".

Modeling Real Inorganic Membranes

The discussion above has concentrated on defect-free nanoporous crystals. These crystals are important in describing materials in real applications, but additional complications exist to develop truly quantitative models of these applications. Here, I briefly mention several factors that must be considered in bridging the gap between these two areas. Practical crystalline inorganic

membranes typically consist of a thin film grown onto a macroporous support, with the latter providing mechanical stability. The characteristics of this support and the presence or absence of a sweep gas in the operating membrane can influence device performance.[47] Real membranes are almost invariably polycrystalline. Describing the influence of the membrane microstructure on the membrane performance remains challenging.[67] Finally, the net mass transfer resistance of a single crystal is a combination of resistances from diffusion inside the crystal and resistances associated with transport into or out of the pores of the crystal.[68] Although the latter resistances are negligible in some situations, they may be in important in applications involving extremely small crystals[69] or when pore mouths are deliberately modified.[70]

Concluding Remarks

This Account has described how MD simulations of adsorbed molecules can complement experiments for understanding macroscopic diffusion in nanopores, especially for chemical mixtures. I conclude by very briefly commenting on limitations of MD simulations and directions for future work. MD simulations are difficult for slow diffusion,[71] although transition-state theory approaches can reduce this limitation.[72] Applications of MD to macroscopic diffusion in nanopores have to date focused on chemically homogeneous and crystallographically ordered materials, but many other interesting materials exist. Most zeolites have framework substitutions that make them chemically heterogeneous.[2,9] Pores in protein crystals are chemically heterogeneous.[73] The disordered pores in nanoporous carbons have many potential applications.[74] These materials represent both a challenge and an opportunity for the MD methods outlined here and other theoretical methods.

This work was supported by the NSF, PRF, DOE, Dreyfus, and Sloan Foundations. I am grateful to the talented researchers who have worked with me (A. Skoulidas, H. Chen, D. Newsome, C. Shang-Shan, and P. Kamakoti) and to my experimental and theoretical collaborators (J. K. Johnson, R. Noble, J. Falconer, H. Jobic, R. Krishna, D. Kohen, and S. Bhatia). It has been a particular pleasure to discuss diffusion with my father, C. A. Sholl.[75]

References

(1) Yang, R. T. *Gas Separation by Adsorption Processes*; Butterworth: Boston, MA, 1987.
(2) Kärger, J.; Ruthven, D. *Diffusion in Zeolites and Other Microporous Materials*; John Wiley and Sons: New York, 1992.
(3) Keil, F. J.; Krishna, R.; Coppens, M. O. Modeling of diffusion in zeolites. *Rev. Chem. Eng.* **2000**, *16*, 71−197.
(4) Jobic, H. Neutron scattering methods for the study of zeolites. *Curr. Opin. Solid State Mater.* **2002**, *6*, 415−422.
(5) Tsapatsis, M.; Gavalas, G. R. Synthesis of porous inorganic membranes. *MRS Bull.* **1999**, *24*, 30−35.
(6) Freeman, B. D. Basis of permeability/selectivity tradeoff relations in polymeric gas separation membranes. *Macromolecules* **1999**, *32*, 375−380.
(7) Hsieh, H. P. *Inorganic Membranes for Separation and Reaction*; Elsevier: Amsterdam, The Netherlands, 1996.
(8) Cussler, E. L. *Multicomponent Diffusion*; Elsevier: Amsterdam, The Netherlands, 1976.
(9) Coppens, M. O.; Bell, A. T.; Chakraborty, A. K. Dynamic Monte Carlo and mean-field study of the effect of strong adsorption sites on self-diffusion in zeolites. *Chem. Eng. Sci.* **1999**, *54*, 3455−3463.
(10) Paschek, D.; Krishna, R. Kinetic Monte Carlo simulations of transport diffusivities of binary mixtures in zeolites. *Phys. Chem. Chem. Phys.* **2001**, *3*, 3185−3191.
(11) Kamakoti, P.; Morreale, B. D.; Ciocco, M. V.; Howard, B. H.; Killmeyer, R. P.; Cugini, A. V.; Sholl, D. S. Prediction of hydrogen flux through sulfur-tolerant binary alloy membranes. *Science* **2005**, *307*, 569−573.
(12) Theodorou, D. N.; Snurr, R. Q.; Bell, A. T. In *Comprehensive Supramolecular Chemistry*; Alberti, G., Bein, T., Eds.; Pergamon Press: New York, 1996; Vol. 7; pp 507−548.
(13) McQuarrie, D. A. *Statistical Mechanics*; Harper and Row: New York, 1975.
(14) Skoulidas, A. I.; Sholl, D. S. Direct tests of the Darken approximation for molecular diffusion in zeolites using equilibrium molecular dynamics. *J. Phys. Chem. B* **2001**, *105*, 3151−3154.
(15) Darken, L. S. Diffusion, mobility and their interrelation through free energy in binary metallic systems. *Trans. Am. Inst. Min., Metall. Pet. Eng.* **1948**, *175*, 184−201.
(16) Dubbeldam, D.; Calero, S.; Vlugt, T. J. H.; Krishna, R.; Maesen, T. L. M.; Smit, B. United atom force field for alkanes in nanoporous materials. *J. Phys. Chem. B* **2004**, *108*, 12301−12313.
(17) Dubbeldam, D.; Calero, S.; Vlugt, T. J. H.; Krishna, R.; Maesen, T. L. M.; Smit, B. Force field parametrization through fitting on inflection points in isotherms. *Phys. Rev. Lett.* **2004**, *93*, 088302.
(18) Chen, H.; Sholl, D. S. Efficient simulation of binary adsorption isotherms using transition matrix Monte Carlo. *Langmuir* **2006**, *22*, 709−716.
(19) Frenkel, D.; Smit, B. *Understanding Molecular Simulation: From Algorithms to Applications*; Academic Press: London, U.K., 2002.
(20) Maginn, E. J.; Bell, A. T.; Theodorou, D. N. Transport diffusivity of methane in silicalite from equilibrium and non-equilibrium simulations. *J. Phys. Chem.* **1993**, *97*, 4173−4181.
(21) Mori, H. Transport collective motion and Brownian motion. *Prog. Theor. Phys.* **1965**, *33*, 423.
(22) Arya, G.; Chang, H. C.; Maginn, E. J. A critical comparison of equilibrium, non-equilibrium and boundary-driven molecular dynamics techniques for studying transport in microporous materials. *J. Chem. Phys.* **2001**, *115*, 8112−8124.
(23) Chempath, S.; Krishna, R.; Snurr, R. Q. Nonequilibrium molecular dynamics simulations of diffusion of binary mixures containing short *n*-alkanes in faujasite. *J. Phys. Chem. B* **2004**, *108*, 13481−13491.
(24) Chong, S.-S.; Jobic, H.; Plazanet, M.; Sholl, D. S. Concentration dependence of transport diffusion of ethane in silicalite: A comparison between neutron scattering experiments and atomically-detailed simulations. *Chem. Phys. Lett.* **2005**, *408*, 157−161.
(25) Jobic, H.; Skoulidas, A. I.; Sholl, D. S. Determination of concentration dependent transport diffusivity of CF_4 in silicalite by neutron scattering experiments and molecular dynamics simulations. *J. Phys. Chem. B* **2004**, *108*, 10613−10616.
(26) Jobic, H.; Bee, M.; Kearley, G. J. Dynamics of ethane and propane in zeolite ZSM-5 studied by quasi-elastic neutron scattering. *Zeolites* **1992**, *12*, 146.
(27) Heink, W.; Karger, J.; Pfeifer, H.; Daterna, K. P.; Nowak, A. K. High-temperature pulsed-field gradient nuclear magnetic resonance self-diffusion measurements of *n*-alkanes in MFI-type zeolites. *J. Chem. Soc., Faraday Trans.* **1992**, *88*, 3505−3509.
(28) Talu, O.; Sun, M. S.; Shah, D. B. Diffusivities of *n*-alkanes in silicalite by steady-state single-crystal membrane technique. *AIChE J.* **1998**, *44*, 681−694.
(29) Skoulidas, A. I.; Sholl, D. S. Transport diffusivities of CH_4, CF_4, He, Ne, Ar, Xe, and SF_6 in silicalite from atomistic simulations. *J. Phys. Chem. B* **2002**, *106*, 5058−5067.
(30) Skoulidas, A. I.; Sholl, D. S. Molecular dynamics simulations of self-diffusivities, corrected diffusivities, and transport diffusivities of light gases in four silica zeolites to assess influences of pore shape and connectivity. *J. Phys. Chem. A* **2003**, *107*, 10132−10141.
(31) Tunca, C.; Ford, D. M. A transition-state theory approach to adsorbate dynamics at arbitrary loadings. *J. Chem. Phys.* **1999**, *111*, 2751−2760.
(32) Hahn, K.; Karger, J.; Kukla, V. Single-file diffusion observation. *Phys. Rev. Lett.* **1996**, *76*, 2762−2765.
(33) Sholl, D. S.; Fichthorn, K. A. Normal, single-file, and dual-mode diffusion of binary adsorbate mixtures in $AlPO_4$-5. *J. Chem. Phys.* **1997**, *107*, 4384−4389.
(34) Sholl, D. S.; Fichthorn, K. A. Concerted diffusion of molecular clusters in a molecular sieve. *Phys. Rev. Lett.* **1997**, *79*, 3569−3572.
(35) van Baten, J. M.; Krishna, R. Entropy effects in adsorption and diffusion of alkane isomers in mordenite: An investigation using CBMC and MD simulations. *Microporous Mesoporous Mater.* **2005**, *84*, 179−191.

(36) Krishna, R.; van Baten, J. M. Diffusion of alkane mixtures in zeolites: Validating the Maxwell−Stefan formulation using MD simulations. *J. Phys. Chem. B* **2005**, *109*, 6386-6396.
(37) Krishna, R.; van Baten, J. M. Influence of isotherm inflection on the diffusivities of C5−C8 linear alkanes in MFI zeolite. *Chem. Phys. Lett.* **2005**, *407*, 159−165.
(38) Papadopoulos, G. K.; Jobic, H.; Theodorou, D. N. Transport diffusivity of N_2 and CO_2 in silicalite: Coherent quasielastic neutron scattering measurements and molecular dynamics simulations. *J. Phys. Chem. B* **2004**, *108*, 12748−12756.
(39) Papadopoulos, G. K. Diffusivity of CH_4 in model silica nanopores: Molecular dynamics and quasichemical mean field theory. *Mol. Simul.* **2005**, *31*, 57−66.
(40) Wesselingh, J. A.; Krishna, R. *Mass Transfer in Multicomponent Mixtures*; Delft University Press: Delft, The Netherlands, 2000.
(41) Duncan, J. B.; Toor, H. L. An experimental study of three component gas diffusion. *AIChE J.* **1962**, *8*, 38−41.
(42) Krishna, R.; van den Broeke, L. J. P. The Maxwell−Stefan description of mass-transport across zeolite membranes. *Chem. Eng. J.* **1995**, *57*, 155−162.
(43) Skoulidas, A. I.; Sholl, D. S.; Krishna, R. Correlation effects in diffusion of CH_4/CF_4 mixtures in MFI zeolite. A study linking MD simulations with the Maxwell−Stefan formulation. *Langmuir* **2003**, *19*, 7977−7988.
(44) Sanborn, M. J.; Snurr, R. Q. Diffusion of binary mixtures of CF_4 and *n*-alkanes in faujasite. *Sep. Purif. Technol.* **2000**, *20*, 1−13.
(45) Sanborn, M. J.; Snurr, R. Q. Predicting membrane flux of CH_4 and CF_4 mixtures in faujasite from molecular simulations. *AIChE J.* **2001**, *47*, 2032−2041.
(46) Skoulidas, A. I.; Sholl, D. S.; Bowen, T. C.; Doelling, C.; Falconer, J. L.; Noble, R. D. Comparing atomistic simulations and experimental measurements for CH_4/CF_4 mixture permeation through silicalite membranes. *J. Membrane Sci.* **2003**, *227*, 123−136.
(47) Skoulidas, A. I.; Sholl, D. S. Multiscale models of sweep gas and porous support effects on zeolite membranes. *AIChE J.* **2005**, *51*, 867−877.
(48) Heuchel, M.; Snurr, R. Q.; Buss, E. Adsorption of $CH_4−CF_4$ mixtures in silicalite: Simulation, experiment, theory. *Langmuir* **1997**, *13*, 6795−6804.
(49) Sholl, D. S. Testing predictions of macroscopic binary diffusion coefficients using lattice models with site heterogeneity. *Langmuir* **2006**, in press.
(50) Mao, Z. G.; Sinnott, S. B. A computational study of molecular diffusion and dynamic flow through carbon nanotubes. *J. Phys. Chem. B* **2000**, *104*, 4618−4624.
(51) Skoulidas, A. I.; Ackerman, D. M.; Johnson, J. K.; Sholl, D. S. Rapid transport of gases in carbon nanotubes. *Phys. Rev. Lett.* **2002**, *89*, 185901.
(52) Chen, H.; Sholl, D. S. Rapid diffusion of CH_4/H_2 mixtures in single-walled carbon nanotubes. *J. Am. Chem. Soc.* **2004**, *126*, 7778−7779.
(53) Sokhan, V. P.; Nicholson, D.; Quirke, N. Fluid flow in nanopores: Accurate boundary conditions for carbon nanotubes. *J. Chem. Phys.* **2002**, *117*, 8531.
(54) Ackerman, D. M.; Skoulidas, A. I.; Sholl, D. S.; Johnson, J. K. Diffusivities of Ar and Ne in carbon nanotubes. *Mol. Simul.* **2003**, *29*, 677−684.
(55) Chen, H.; Sholl, D. S. Predictions of selectivity and flux for single-walled carbon nanotubes and membranes. *J. Membrane Sci.* **2006**, *269*, 152−160.
(56) Skoulidas, A. I.; Sholl, D. S.; Johnson, J. K. Adsorption and diffusion of carbon dioxide and nitrogen through single walled carbon nanotube membranes. *J. Chem. Phys.* **2006**, *124*, 054708.
(57) Wei, X.; Srivastava, S. Theory of transport of long polymer molecules through carbon nanotube channels. *Phys. Rev. Lett.* **2003**, *91*, 235901.
(58) Bhatia, S. K.; Chen, H.; Sholl, D. S. Comparisons of diffusive and viscous contributions to transport coefficients of light gases in single-walled carbon nanotubes. *Mol. Simul.* **2005**, *31*, 643−649.
(59) Jakobtorweihen, S.; Verbeek, M. G.; Lowe, C. P.; Keil, F. J.; Smit, B. Understanding the loading dependence of self-diffusion in carbon nanotubes. *Phys. Rev. Lett.* **2005**, *95*, 044501.
(60) Chen, H.; Johnson, J. K.; Sholl, D. S. Transport diffusion of gases is rapid in flexible carbon nanotubes. *J. Phys. Chem. B* **2006**, *110*, 1971−1975.
(61) Hinds, B. J.; Chopra, N.; Rantell, T.; Andrews, R.; Gavalas, V.; Bachas, L. Aligned multiwalled carbon nanotube membranes. *Science* **2004**, *303*, 62−65.
(62) Majumder, M.; Chopra, N.; Andrews, R.; Hinds, B. J. Enhanced flow in carbon nanotubes. *Nature* **2005**, *438*, 44.
(63) Yaghi, O. M.; O'Keeffe, M.; Ockwig, N. W.; Chae, H. K.; Eddaoudi, M.; Kim, J. Reticular synthesis and the design of new materials. *Nature* **2003**, *423*, 705−714.
(64) Duren, T.; Sarkisov, L.; Yaghi, O. M.; Snurr, R. Q. Design of new materials for methane storage. *Langmuir* **2004**, *20*, 2683−2689.
(65) Skoulidas, A. I.; Sholl, D. S. Self-diffusion and transport diffusion of light gases in metal-organic framework materials assessed using molecular dynamics simulations. *J. Phys. Chem. B* **2005**, *109*, 15760−15768.
(66) Sarkisov, L.; Duren, T.; Snurr, R. Q. Molecular modeling of adsorption in novel nanoporous metal-organic materials. *Mol. Phys.* **2004**, *102*, 211−221.
(67) Snyder, M. A.; Lai, Z.; Tsapatsis, M.; Vlachos, D. G. Combining simultaneous reflectance and fluorescence imaging with SEM for conclusive identification of polycrystalline features of MFI membranes. *Microporous Mesoporous Mater.* **2004**, *76*, 29−33.
(68) Newsome, D. A.; Sholl, D. S. Predictive assessment of surface resistances in zeolite membranes using atomically-detailed models. *J. Phys. Chem. B* **2005**, *109*, 7237−7244.
(69) Song, W.; Justice, R. E.; Jones, C. A.; Grassian, V. H.; Larsen, S. C. Synthesis, characterization, and adsorption properties of nanocrystalline ZSM-5. *Langmuir* **2004**, *20*, 8301−8306.
(70) Hong, M.; Falconer, J. L.; Noble, R. D. Modification of zeolite membranes for H_2 separation by catalytic cracking of methyldiethoxysilane. *Ind. Eng. Chem. Res.* **2005**, *44*, 4035−4041.
(71) Ramanan, H.; Auerbach, S. M.; Tsapatsis, M. Beyond lattice models of activated transport in zeolites: High-temperature molecular dynamics of self-diffusion and cooperative diffusion of benzene in NaX. *J. Phys. Chem. B* **2004**, *108*, 17171−17178.
(72) Beerdsen, E.; Dubbeldam, D.; Smit, B. Molecular understanding of diffusion in confinement. *Phys. Rev. Lett.* **2005**, *95*, 164505.
(73) Malek, K.; Odijk, T.; Coppens, M. O. Diffusion in protein crystals—A computer simulation. *ChemPhysChem* **2004**, *5*, 1596−1599.
(74) Gogotsi, Y.; Nikitin, A.; Ye, H. H.; Zhou, W.; Fischer, J. E.; Bo, Y.; Foley, H. C.; Barsoum, M. W. Nanoporous carbide-derived carbon with tunable pore size. *Nat. Mater.* **2003**, *2*, 591−594.
(75) Bhatia, B.; Luo, X. J.; Sholl, C. A.; Sholl, D. S. Diffusion of hydrogen in cubic Laves phase $HfTi_2H_x$. *J. Phys. Condens. Matter* **2004**, *16*, 8891−8903.

AR0402199